2012

# Very high data rate MB-OFDM UWB systems with transmit diversity techniques

Ngoc Phuc Le
*University Of Wollongong*, pnl750@uowmail.edu.au

Le Chung Tran
*University of Wollongong*, lctran@uow.edu.au

Farzad Safaei
*University of Wollongong*, farzad@uow.edu.au

# Very high data rate MB-OFDM UWB systems with transmit diversity techniques


## Abstract

In this paper, the application of space time block codes in a very high data rate multiband-OFDM ultra-wideband (VHDR MB-OFDM UWB) system, where the Modified Dual Carrier Modulation (MDCM) scheme and Low Density Parity Check codes are deployed, is investigated. First, we present a new table-based mapping approach and derive soft-demapping expressions for the MDCM scheme. We then propose a space-time-frequency coded VHDR MB-OFDM UWB system by incorporating space time block codes into the conventional VHDR MB-OFDM UWB system. Numerical simulations of the system supporting a data rate of 1Gbps over the IEEE 802.15.3a channel models are implemented. The simulation results confirm the new mapping/demapping method as well as demonstrate the significant improvement in terms of packet error rate performance of the proposed system over the standard one.



## Keywords

techniques, transmit, diversity, high, rate, mb, ofdm, uwb, data, very, systems


## Disciplines

Engineering | Science and Technology Studies


## Publication Details

Le, N. Phuc., Tran, L. Chung. & Safaei, F. (2012). Very high data rate MB-OFDM UWB systems with transmit diversity techniques. In L. Tran (Eds.), 12nd IEEE International Symposium on Communications and Information Technologies (ISCIT 2012) (pp. 508-512). Australia: IEEE.

# Very High Data Rate MB-OFDM UWB Systems with Transmit Diversity Techniques

Ngoc Phuc Le, Le Chung Tran, Farzad Safaei
School of Electrical, Computer and Telecommunications Engineering
The University of Wollongong
Northfields Avenue, NSW 2522, Australia
Emails: {pnl750, lctran, farzad}@uow.edu.au

*Abstract*— **In this paper, the application of space time block codes in a very high data rate multiband-OFDM ultra-wideband (VHDR MB-OFDM UWB) system, where the Modified Dual Carrier Modulation (MDCM) scheme and Low Density Parity Check codes are deployed, is investigated. First, we present a new table-based mapping approach and derive soft-demapping expressions for the MDCM scheme. We then propose a space-time-frequency coded VHDR MB-OFDM UWB system by incorporating space time block codes into the conventional VHDR MB-OFDM UWB system. Numerical simulations of the system supporting a data rate of 1Gbps over the IEEE 802.15.3a channel models are implemented. The simulation results confirm the new mapping/demapping method as well as demonstrate the significant improvement in terms of packet error rate performance of the proposed system over the standard one.**

***Keywords- MB-OFDM UWB; MDCM; LDPC; Alamouti code; IEEE 802.15.3a channel models***

## I. INTRODUCTION

Ultra-wideband (UWB) wireless communications have emerged as one of the most promising transmission techniques for high data rate applications with low cost and low power consumption [1], [2]. On the other hand, Multiple Input Multiple Output (MIMO) techniques, e.g. space time codes [3], [4], could significantly improve system performance. Therefore, the combination of these technologies may be a potential solution for satisfying the demand of future personal wireless applications.

The investigation of space time frequency (STF) coded multiband-orthogonal frequency division multiplexing ultra-wideband (MB-OFDM UWB) systems have been mentioned in the literature, such as [5] and [6]. In [5], the authors proposed a coding framework for MIMO MB-OFDM UWB systems. They quantified the system performance regardless of specific coding schemes in the case of Nakagami-*m* frequency selective fading channels. The authors in [6] examined the performance and derived the design criteria for STF codes in the proposed STF coded MB-OFDM UWB system under the channels with the log-normal distribution. Although the results in terms of performance improvement are promising, these works only considered the systems with hard-demapping.

As introduced in the WiMedia's latest Release 1.5 [7], for the case of very high data rate (VHDR) applications, the Modified Dual Carrier Modulation (MDCM) and Low Density Parity Check (LDPC) codes are deployed, replacing a DCM modulation and convolutional codes. Therefore, in these configurations, a MDCM soft-demapping process is required to produce soft-values for the input of the LDPC decoder.

In this paper, we examine the application of space time block codes (STBCs) in the VHDR MB-OFDM UWB system. First, we propose a table-based mapping and derive soft-demapping expressions for the MDCM scheme. Next, we consider enhancing the performance of the standard system with transmit diversity techniques. Specifically, we propose a Space-Time-Frequency coded VHDR MB-OFDM UWB system by incorporating STBCs into the standard VHDR MB-OFDM UWB system. It will be shown via simulations that the proposed system could achieve a significant improvement in performance compared to the conventional one.

The rest of the paper is organized as follows. In Section II, we review the WiMedia's VHDR MB-OFDM specifications, and then describe the mapping/demapping method for the MDCM. In Section III, we propose the STFC VHDR MB-OFDM UWB system. Simulation results are provided in Section IV. Finally, Section V concludes the paper.

*Notation:* A bold letter denotes a vector or a matrix, whereas an italic letter denotes a variable. $(.)^*$, and $(\bullet)$ denote complex conjugation, and the Hadamard product, respectively. $\tilde{a}$ denotes an estimation of $a$. *Re{.}* and *Im{.}* refer to the real and imaginary parts of a complex number, respectively.

## II. VERY HIGH DATA RATE MB-OFDM UWB SYSTEMS

### A. Overview of WiMedia's VHDR MB-OFDM UWB PHY

In the MB-OFDM approach [7], the entire UWB spectrum between 3.1-10.6 GHz is divided into 14 subbands, each has a

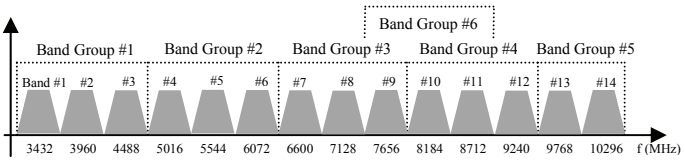


Fig. 1 MB-OFDM band group allocation

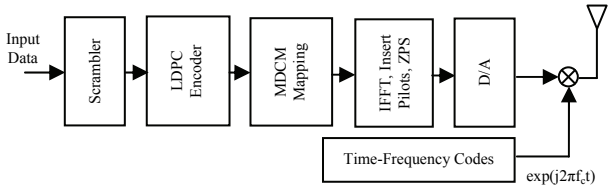


Fig. 2 Transmit architecture for a VHDR MB-OFDM system

bandwidth of 528 MHz. These subbands are grouped into 6 band groups as shown in Fig. 1.

The physical layer architecture of a VHDR MB-OFDM system is similar to that of a conventional OFDM one, except that the carrier frequency changes from one symbol to another. The block diagram of the transmitter is depicted in Fig. 2. Accordingly, information data are first scrambled, and then encoded by a LDPC encoder [8]. The encoded bit stream is mapped into a MDCM constellation. The resulting data are fed into an IFFT blocks to generate OFDM symbols. The total number of subcarriers in each OFDM symbol is 128, of which, there are 100 data subcarriers, 12 pilot subcarriers, 10 guard subcarriers, and the rest are null subcarriers. At the receiver, the signals are processed in the reverse order.

With respect to some characteristics the VHDR MB-OFDM system differs from the conventional OFDM system. First, a zero-padded suffix (ZPS) of length 37 is used to mitigate the effects of multipath as well as provide a guard interval for transceivers to switch from one subband to another. Second, the MB-OFDM system transmits symbols using different subbands specified by time-frequency codes (TFCs). These TFCs are used not only for providing frequency diversity but also for multiple access purpose. Third, wireless channels in a MB-OFDM UWB system follow a log-normal distribution, rather than the Rayleigh distribution.

### *B. A proposed table-based mapping approach for MDCM*

For the MDCM modulation, each group of eight bits is converted into two complex numbers, i.e. two OFDM subcarriers, $x(k)$ and $x(k+50)$, $k \in [0,49]$. The mapping process is mathematically described in the WiMedia's specifications [7]. By exploiting the structure of the MDCM mapping, we propose another way of mapping by using Table I. This mapping table is arranged in a compact way so that it has only 16 rows instead of 256 ones as normally for binary 8-tuples. The mapping process is described as follows.

TABLE I. A PROPOSED MAPPING TABLE FOR MDCM.

| No | $b_0b_1\,b_2\,b_3\,b_4b_5\,b_6\,b_7$ | $Re\{x_k\}$ | $Im\{x_k\}$ | $Re\{x_{k+50}\}$ | $Im\{x_{k+50}\}$ |
|---|---|---|---|---|---|
| 1 | 0 0 0 0 0 0 0 0 | -15 | -15 | 9 | 9 |
| 2 | 0 0 0 0 0 0 1 0 1 | -13 | -13 | 1 | 1 |
| 3 | 0 0 0 0 0 1 1 1 1 | -11 | -11 | -7 | -7 |
| 4 | 0 0 0 0 0 1 0 1 0 | -9 | -9 | -15 | -15 |
| 5 | 0 1 0 1 0 0 0 0 0 | -7 | -7 | 11 | 11 |
| 6 | 0 1 0 1 0 1 0 1 | -5 | -5 | 3 | 3 |
| 7 | 0 1 0 1 1 1 1 1 | -3 | -3 | -5 | -5 |
| 8 | 0 1 0 1 1 0 1 0 | -1 | -1 | -13 | -13 |
| 9 | 1 1 1 1 0 0 0 0 | 1 | 1 | 13 | 13 |
| 10 | 1 1 1 1 0 1 0 1 | 3 | 3 | 5 | 5 |
| 11 | 1 1 1 1 1 1 1 1 | 5 | 5 | -3 | -3 |
| 12 | 1 1 1 1 1 0 1 0 | 7 | 7 | -11 | -11 |
| 13 | 1 0 1 0 0 0 0 0 | 9 | 9 | 15 | 15 |
| 14 | 1 0 1 0 0 1 0 1 | 11 | 11 | 7 | 7 |
| 15 | 1 0 1 0 1 1 1 1 | 13 | 13 | -1 | -1 |
| 16 | 1 0 1 0 1 0 1 0 | 15 | 15 | -9 | -9 |

Denote a group of 8 bits needed to be mapped to be $b_0b_1b_2b_3b_4b_5b_6b_7$. The value of the bits $b_0b_1b_4b_5$ will determine the row from which the real parts of $x(k)$ and $x(k+50)$ should be selected. Meanwhile, the imaginary parts will be determined by the value of the bits $b_2b_3b_6b_7$. We now take a group of 8 bits $(11001010)$ as an example. The value $b_0b_1b_4b_5 = (1110)$ will be corresponding to the 12th row. Hence, we have $Re\{x(k)\} = 7$ and $Re\{x(k+50)\} = -11$. Similarly, for the bits $b_2b_3b_6b_7 = (0010)$, by looking up to the 4th row, we have $Im\{x(k)\} = -9$ and $Im\{x(k+50)\} = -15$. Therefore, the values $x(k)$ and $x(k+50)$ are $(7-9j)$ and $(-11-15j)$, respectively. This mapping approach will help to implement mapping and demapping quickly. Also, a direct relation between constellation values and their corresponding bits shown in this table will be very useful for deriving soft-demapping expressions.

We have some important observations from the above mapping. First, the values $Re\{x(k)\}$ and $Re\{x(k+50)\}$ depend only on the bits $b_0, b_1, b_4, b_5$, whereas the values $Im\{x(k)\}$ and $Im\{x(k+50)\}$ depend only on the bits $b_2, b_3, b_6, b_7$. Therefore, the computation of $\tilde{b}_i$, $i = 0,1,4,5$, depends only on $Re\{\tilde{x}(k)\}$ and $Re\{\tilde{x}(k+50)\}$. Likewise, the computation of $\tilde{b}_i$, $i = 2,3,6,7$, depends on $Im\{\tilde{x}(k)\}$ and $Im\{\tilde{x}(k+50)\}$. Second, the relation between the bits $b_0, b_1, b_4, b_5$ and $Re\{x(k)\}$ is exactly the same as that between the bits $b_2, b_3, b_6, b_7$ and $Im\{x(k)\}$. Also, the relation between the bits $b_0, b_1, b_4, b_5$ and $Re\{x(k+50)\}$ is similar to that between the bits $b_2, b_3, b_6, b_7$ and $Im\{x(k+50)\}$. Consequently, the steps required to obtain $\tilde{b}_i$, $i = 0,1,4,5$, from

$Re\{\tilde{x}(k)\}$ and $Re\{\tilde{x}(k+50)\}$ is exactly the same as those needed to get $\tilde{b}_i, i = 2,3,6,7,$ from $Im\{\tilde{x}(k)\}$ and $Im\{\tilde{x}(k+50)\}$. These observations are similar to DCM in [9].

### C. Derivation of soft-demapping expressions for MDCM

We now derive MDCM soft-demapping expressions. Denote the signal received at the $k^{\text{th}}$ subcarrier to be $y(k)$,

$$y(k) = h(k)x(k) + n(k), \tag{1}$$

where $h(k)$ is the complex fading coefficient and $n(k)$ is a complex Gaussian random variable with variance $\sigma^2$ per dimension. The equalized signal could be expressed as

$$\tilde{x}(k) = y(k)h^*(k) = |h(k)|^2 x(k) + n(k)h^*(k), \tag{2}$$

where the noise term has variance $|h(k)|^2\sigma^2$ per dimension. The demapping problem is that we need to estimate $\tilde{b}_i, i = 0,1,...,7,$ given signals $\tilde{x}(k)$ and $\tilde{x}(k+50)$.

Define the log-likelihood ratio (LLR) of the $i^{\text{th}}$, $i = 0,...,7$ bit associated to a pair of symbols $x(k)$ and $x(k+50)$ as

$$\text{LLR}(b_i) = \log\frac{\Pr[b_i = 1 \mid h(k), h(k+50), \tilde{x}(k), \tilde{x}(k+50)]}{\Pr[b_i = 0 \mid h(k), h(k+50), \tilde{x}(k), \tilde{x}(k+50)]}. \tag{3}$$

Using the first observation mentioned in Section II.B, for estimating bits $\tilde{b}_i, i = 0,1,4,5,$ we could express the LLR values as in (4) (see at the bottom), where $S_i^{(0)}$ and $S_i^{(1)}$ are the sets of the real parts of constellation symbols whose $i^{\text{th}}$ bit is 0 and 1, respectively. As the two subcarriers, $k^{\text{th}}$ and $(k+50)^{\text{th}}$, are separated by at least 200MHz in UWB systems [7], it is possible to assume that $\tilde{x}(k)$ and $\tilde{x}(k+50)$ are independent. Assume that all the symbols are equally likely, by applying the property of a joint Gaussian probability function (pdf) and Bayes' rule, we have (5), where the joint Gaussian pdf $f\{.\}$ could be expressed by (6), (7) [10]. Using the log-map approximation, we finally have (8). Based on the second observation in Section II.B, the LLR values for bits $\tilde{b}_i, i = 2,3,6,7$ are obtained by replacing $Re\{\tilde{x}(k)\}$ and $Re\{\tilde{x}(k+50)\}$ in (8) with $Im\{\tilde{x}(k)\}$ and $Im\{\tilde{x}(k+50)\}$, respectively. Note that $S_i^{(0)}$ and $S_i^{(1)}$ are now the corresponding sets of the imaginary parts of symbols.

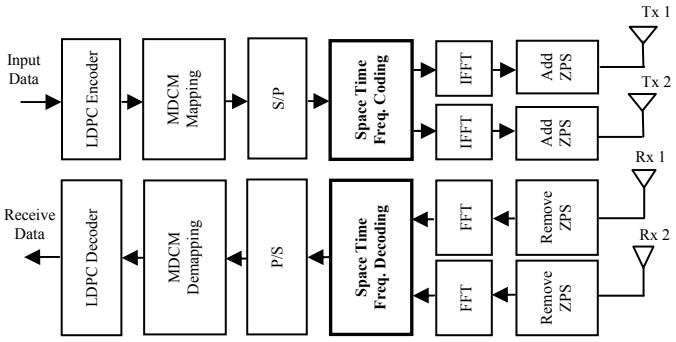


Fig. 3 Block diagram of the proposed STF VHDR MB-OFDM UWB system

## III. STF CODED VHDR MB-OFDM UWB SYSTEM

In this section, we propose the Space-Time-Frequency coded VHDR MB-OFDM UWB system. We consider a system equipped with $M = 2$ transmit antennas and $N$ receive antennas. A simplified block diagram of this system is depicted in Fig. 3. The operation of this system is described below.

At the transmitter, the data bits are encoded, and mapped onto MDCM constellation points. The resulting signal is then fed into the space-time-frequency encoder. At the encoder, the Alamouti code [4] is used for implementing the STF encoding. Denote $\mathbf{x}_m = [x_m(0),...,x_m(K-1)], m = 1,2,$ to be the two blocks of $K = 100$ complex numbers that the encoder takes for each

$$\text{LLR}(b_i) = \log\left(\frac{\sum_{(\alpha_1,\alpha_2)\in S_i^{(1)}} \Pr[\text{Re}\{x(k)\} = \alpha_1, \text{Re}\{x(k+50)\} = \alpha_2 \mid h(k), h(k+50), \text{Re}\{\tilde{x}(k)\}, \text{Re}\{\tilde{x}(k+50)\}]}{\sum_{(\beta_1,\beta_2)\in S_i^{(0)}} \Pr[\text{Re}\{x(k)\} = \beta_1, \text{Re}\{x(k+50)\} = \beta_2 \mid h(k), h(k+50), \text{Re}\{\tilde{x}(k)\}, \text{Re}\{\tilde{x}(k+50)\}]}\right) \tag{4}$$

$$\text{LLR}(b_i) = \log\left(\frac{\sum_{(\alpha_1,\alpha_2)\in S_i^{(1)}} f_\alpha\{\text{Re}\{\tilde{x}(k)\}, \text{Re}\{\tilde{x}(k+50)\} \mid h(k), h(k+50), \text{Re}\{x(k)\} = \alpha_1, \text{Re}\{x(k+50)\} = \alpha_2\}}{\sum_{(\beta_1,\beta_2)\in S_i^{(0)}} f_\beta\{\text{Re}\{\tilde{x}(k)\}, \text{Re}\{\tilde{x}(k+50)\} \mid h(k), h(k+50), \text{Re}\{x(k)\} = \beta_1, \text{Re}\{x(k+50)\} = \beta_2\}}\right) \tag{5}$$

$$f_\alpha\{.\} = \frac{1}{2\pi |h(k)||h(k+50)|\sigma^2}\exp\left(-\frac{[\text{Re}\{\tilde{x}(k)\} - |h(k)|^2\alpha_1]^2}{2|h(k)|^2\sigma^2} - \frac{[\text{Re}\{\tilde{x}(k+50)\} - |h(k+50)|^2\alpha_2]^2}{2|h(k+50)|^2\sigma^2}\right) \tag{6}$$

$$f_\beta\{.\} = \frac{1}{2\pi |h(k)||h(k+50)|\sigma^2}\exp\left(-\frac{[\text{Re}\{\tilde{x}(k)\} - |h(k)|^2\beta_1]^2}{2|h(k)|^2\sigma^2} - \frac{[\text{Re}\{\tilde{x}(k+50)\} - |h(k+50)|^2\beta_2]^2}{2|h(k+50)|^2\sigma^2}\right) \tag{7}$$

$$\text{LLR}(b_i) = \frac{1}{2\sigma^2}\left\{\begin{array}{l} -\min\limits_{(\alpha_1,\alpha_2)\in S_i^{(1)}}\left(\frac{[\text{Re}\{\tilde{x}(k)\} - |h(k)|^2\alpha_1]^2}{|h(k)|^2} + \frac{[\text{Re}\{\tilde{x}(k+50)\} - |h(k+50)|^2\alpha_2]^2}{|h(k+50)|^2}\right) + \\ \min\limits_{(\beta_1,\beta_2)\in S_i^{(0)}}\left(\frac{[\text{Re}\{\tilde{x}(k)\} - |h(k)|^2\beta_1]^2}{|h(k)|^2} + \frac{[\text{Re}\{\tilde{x}(k+50)\} - |h(k+50)|^2\beta_2]^2}{|h(k+50)|^2}\right) \end{array}\right\}, i = 0,1,4,5 \tag{8}$$

coding operation. In the first period, the encoder outputs $\mathbf{x}_1$ and $\mathbf{x}_2$ for transmission via the first and second antenna, respectively. In the next period, the two output sequences are $-\mathbf{x}_2^*$ and $\mathbf{x}_1^*$. Therefore, the STF matrix could be expressed as

$$\mathbf{X} = \begin{bmatrix} \mathbf{x}_1 & -\mathbf{x}_2^* \\ \mathbf{x}_2 & \mathbf{x}_1^* \end{bmatrix}. \quad (9)$$

The output sequences from the STF encoder are then fed into 128-point IFFT blocks. The IFFT output is added with a zero-padded suffix (ZPS) to form a MB-OFDM symbol before being transmitted via its corresponding transmit antenna.

At the receiver, the received signal at each antenna is fed into the FFT block after the ZPS is removed. Denote $\mathbf{y}_n^1$ and $\mathbf{y}_n^2$ to be the resulting signals from the $n^{\text{th}}$ receive antenna in the first and second period, respectively. These signals could be expressed as [6]

$$\mathbf{y}_n^1 = \mathbf{H}_{n,1} \bullet \mathbf{x}_1 + \mathbf{H}_{n,2} \bullet \mathbf{x}_2 + \mathbf{N}_n^1, n = 1,2,...,N \quad (10.1)$$

$$\mathbf{y}_n^2 = -\mathbf{H}_{n,1} \bullet \mathbf{x}_2^* + \mathbf{H}_{n,2} \bullet \mathbf{x}_1^* + \mathbf{N}_n^2, n = 1,2,...,N \quad (10.2)$$

where $\mathbf{y}_n^p = [\mathrm{y}_n^p(0),..., \mathrm{y}_n^p(K-1)]$, $p = 1,2; n = 1,2,...,N$ are the received signals, $\mathbf{H}_{n,m} = [H_{n,m}(0), H_{n,m}(1)..., H_{n,m}(K-1)]$ is the channel frequency response of the path between the $m^{\text{th}}$ transmit antenna and the $n^{\text{th}}$ receive antenna, which remains constant during the two consecutive periods of transmission, and $\mathbf{N}_n^p$, $p = 1,2$ are independent noise samples modelled as Gaussian random variables with variance $\sigma^2$ per dimension.

At the STF decoder, assuming perfect channel state information is available, the combined signals, namely $\tilde{\mathbf{x}}_1$ and $\tilde{\mathbf{x}}_2$, are obtained as in (11) (see at the bottom), where $\|.\|^2$ denotes the element-wise absolute square operation, and both the noise terms, $\mathbf{G}_1$ and $\mathbf{G}_2$, are complex Gaussian random variables with variance of $\sigma^2 \sum_{n=1}^{N} \{\| \mathbf{H}_{n,1} \|^2 + \| \mathbf{H}_{n,2} \|^2\} = \sigma^2 \mathbf{A}$ per dimension. These two combined sequences are then taken by the MDCM demapper. The demapper will calculate the soft-value for each bit. Due to the similarity between each element in two vectors, $\tilde{\mathbf{x}}_1$ and $\tilde{\mathbf{x}}_2$ in (11), and the equation (2), the LLR expression used to calculate soft-values in this system are derived in a similar way to the ones in Section II.C. As an example, the LLR expressions used for calculating soft-values of the $i^{\text{th}}$ bit associated with the pair of symbols $x_1(k)$ and $x_1(k+50)$ of $\mathbf{x}_1$ are given in (12), where $\mathbf{A}=[A(0),..., A(k),..., A(K-1)]$. It should be noted that the LLR values, such as in (8) and (12), could be further normalized as done in [11]. Finally, the LDPC decoder takes the soft-values for soft-decoding in order to retrieve the transmitted information.

TABLE II. SIMULATION PARAMETERS.

| Parameter | Value |
|---|---|
| Data rate | 1024 Mbps |
| FFT size | 128 |
| Number of information data subcarriers | 100 |
| Modulation scheme | MDCM and 16-QAM |
| LDPC code (code rate of 4/5) | Table 6.32 in [7] |
| Channel models | CM1, CM2, CM3, CM4 |

## IV. SIMULATION RESULTS

In this section, simulation results are provided to support the derived mapping/demapping method as well as illustrate the performance improvement of the proposed system over the conventional one. The simulation parameters are chosen based on the WiMedia's specifications for the data rate of 1024 Mbps, and are listed in Table II. In addition, the LDPC encoding algorithm developed in [8] which could achieve linear running time is adopted in our simulation. We measure the system performance in terms of packet error rate (PER) over the IEEE 802.15.3a channel models defined in [12]. There are four channel models, namely CM1, CM2, CM3, and CM4, corresponding to different scenarios. The CM1 channel is based on a measurement of a Line of Sight (LOS) scenario where the distance between the transmitter and the receiver is up to 4 m. The others are CM2 (0-4m, Non Line of Sight-NLOS), CM3 (4-10m, NLOS), CM4 (4-10m, NLOS, rms delay spread of 25 ns). Moreover, the multipath gains are modeled as independent log-normally distributed random variables in these models. We assume that perfect channel state information is available at the receiver.

Fig. 4 shows the PER performance of the conventional VHDR MB-OFDM UWB system with the mapping/demapping method presented in Section II. The PER performance of the same system using 16-QAM modulation is also simulated for comparison. It can be seen that, the system performance with MDCM is better than that with 16-QAM, although both of them have the same bandwidth efficiency. This is because the

$$\tilde{\mathbf{x}}_1 = \sum_{n=1}^{N} \{\mathbf{H}_{n,1}^* \bullet \mathbf{y}_n^1 + \mathbf{H}_{n,2} \bullet (\mathbf{y}_n^2)^*\} = \sum_{n=1}^{N} \{\| \mathbf{H}_{n,1} \|^2 + \| \mathbf{H}_{n,2} \|^2\} \bullet \mathbf{x}_1 + \sum_{n=1}^{N} \{\mathbf{N}_n^1 \bullet \mathbf{H}_{n,1}^* + (\mathbf{N}_n^2)^* \bullet \mathbf{H}_{n,2}\} \underset{def}{=} \mathbf{A} \bullet \mathbf{x}_1 + \mathbf{G}_1 \quad (11.1)$$

$$\tilde{\mathbf{x}}_2 = \sum_{n=1}^{N} \{\mathbf{H}_{n,2}^* \bullet \mathbf{y}_n^1 - \mathbf{H}_{n,1} \bullet (\mathbf{y}_n^2)^*\} = \sum_{n=1}^{N} \{\| \mathbf{H}_{n,1} \|^2 + \| \mathbf{H}_{n,2} \|^2\} \bullet \mathbf{x}_2 + \sum_{n=1}^{N} \{\mathbf{N}_n^1 \bullet \mathbf{H}_{n,2}^* - (\mathbf{N}_n^2)^* \bullet \mathbf{H}_{n,1}\} \underset{def}{=} \mathbf{A} \bullet \mathbf{x}_2 + \mathbf{G}_2 \quad (11.2)$$

$$\mathrm{LLR}(b_i) = \frac{1}{2\sigma^2} \left\{ \begin{array}{l} -\min\limits_{(\alpha_1,\alpha_2) \in S_i^{(1)}} \left( \dfrac{[\mathrm{Re}\{\tilde{x}_1(k)\} - A(k)\alpha_1]^2}{A(k)} + \dfrac{[\mathrm{Re}\{\tilde{x}_1(k+50)\} - A(k+50)\alpha_2]^2}{A(k+50)} \right) + \\ \min\limits_{(\beta_1,\beta_2) \in S_i^{(0)}} \left( \dfrac{[\mathrm{Re}\{\tilde{x}_1(k)\} - A(k)\beta_1]^2}{A(k)} + \dfrac{[\mathrm{Re}\{\tilde{x}_1(k+50)\} - A(k+50)\beta_2]^2}{A(k+50)} \right) \end{array} \right\}, i = 0,1,4,5 \quad (12)$$

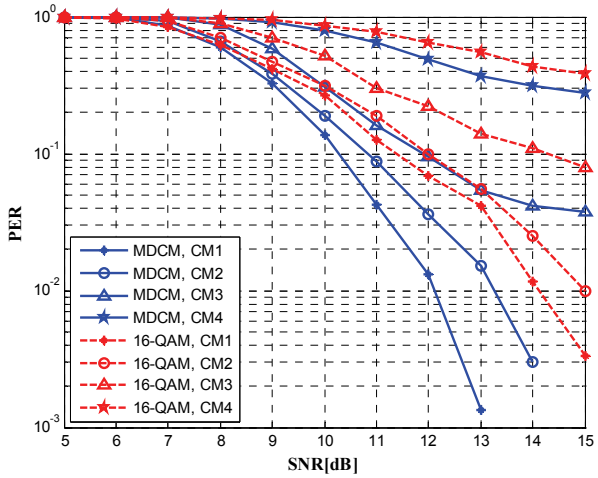


Fig. 4 Performance of the VHDR MB-OFDM UWB system with MDCM and 16-QAM modulation schemes (1 Rx antenna)

MDCM scheme could exploit frequency diversity as the same bits are mapped onto two different subcarriers [7].

The performance of the proposed STFC VHDR MB-OFDM UWB system is shown in Fig. 5 and Fig. 6. In Fig. 5, we compare the PER performance of the proposed system equipped with two transmit antennas and one receiver antenna with that of the conventional system. It is clear that there is a significant improvement in performance over all four channel models. For example, a gain of about 3 dB at PER=$10^{-2}$ could be achieved over the CM1 and CM2 channel models. Similar observations can be made in the case of two receive antennas as depicted in Fig. 6. Moreover, the PER performance of $10^{-2}$ could be attained at low SNR values with this system even in the highly dispersive channel models of CM3 and CM4.

## V. Conclusions

We have examined the application of space time block codes in the VHDR MB-OFDM UWB system. The table-based mapping approach and soft-demapping expressions for MDCM modulation have been introduced. The proposed STFC VHDR MB-OFDM UWB system has been described in detail and its performance has been evaluated via simulations. It can be concluded that the proposed system could achieve a significant improvement in terms of PER performance compared to the conventional one. We have considered the systems equipped with up to two transmit/receive antennas using the effective Alamouti code in this paper. Extending this work to the systems with a higher number of transmit antennas is under investigated for a completed study.

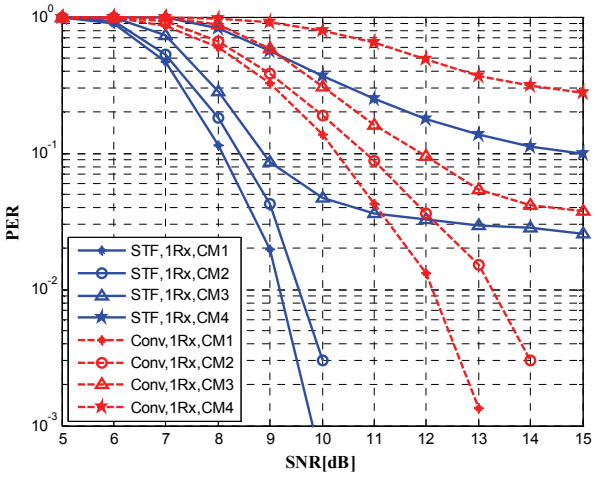


Fig. 5 Performance comparison between the STFC VHDR MB-OFDM UWB system and the conventional system (1 Rx antenna)

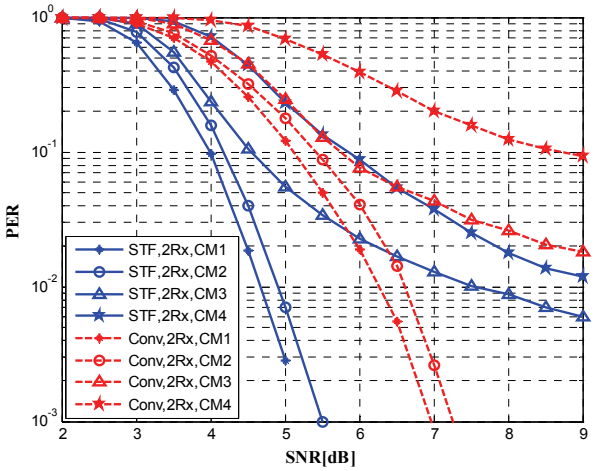


Fig. 6 Performance comparison between the STFC VHDR MB-OFDM UWB system and the conventional system (2 Rx antennas)

## References


[1] L. Yang and G. B. Giannakis, "Ultra-wideband communications: an idea whose time has come, " *IEEE Signal Processing Magazine*, vol. 21, no. 6, pp. 26-54, Nov 2004.

[2] A. Batra, J. Balakrishnan, G. R. Aiello, J. R. Foerster, and A. Dabak, "Design of a multiband OFDM system for realistic UWB channel environments," *IEEE Trans. Microwave Theory Techniques*, vol. 52, no. 9, pp. 2123-2138, Sept. 2004.

[3] V. Tarokh, N. Seshadri, and A. R. Calderbank, "Space-time codes for high data rate wireless communication: performance criterion and code construction," *IEEE Trans. Inform. Theory,* vol. 44, no. 2, pp. 744-765, Mar. 1998.

[4] S. M. Alamouti, "A simple transmit diversity technique for wireless communications," *IEEE Journal on Selected Areas in Communications*, vol. 16, no. 8, pp. 1451- 1458, Oct. 1998.

[5] W. P. Siriwongpairat, W. Su, M. Olfat, and K. J. R. Liu, "Multiband OFDM MIMO coding framework for UWB communication systems," *IEEE Trans. Signal Processing*, vol. 54, no. 1, pp. 214-224, Jan. 2006.

[6] L. C. Tran and A. Mertins, "Space-time frequency code implementation in MB-OFDM UWB communications: design criteria and performance," *IEEE Trans. Wireless Commun.*, vol. 8, no. 2, pp. 701-713, Feb. 2009.

[7] A. Batra *et al.*, "Multiband OFDM physical layer specification," *WiMedia Alliance*, Release 1.5, August 2009.

[8] T. J. Richardson and R. Urbanke, "Efficient encoding of low-density parity-check codes," *IEEE Transactions on Information Theory*, vol. 47, no. 2, pp. 638- 656, Feb. 2001.

[9] V. Srivastava, "Practical algorithms for soft-demapping dual-carrier modulated symbols," in *Proc. IEEE Singapore Int. Conf. on Comm. Systems, ICCS 2006*, pp. 1- 5, Oct. 2006.

[10] S. L. Miller and D. G. Childers, *Probability and random processes: With applications to signal processing and communications*, Elsevier Academic Press, 2004.

[11] F. Tosato and P. Bisaglia, "Simplified soft-output demapper for binary interleaved COFDM with application to HIPERLAN/2," in *Proc. IEEE Int. Conf. Communications*, *ICC 2002*, vol. 2, pp. 664–668, April 2002.

[12] J. Foerster *et al.*, "Channel modeling sub-committee report final," IEEE P802.15-02/490r1-SG3a, Feb. 2003.